SpezialForschungsBereich F 32

Karl–Franzens Universität Graz
Technische Universität Graz
Medizinische Universität Graz

Magnetic Induction Tomography: A feasibility study of brain oedema detection using a finite element human head model

R. Merwa H. Scharfetter

SFB-Report No. 2007–013 December 2007

A–8010 GRAZ, HEINRICHSTRASSE 36, AUSTRIA

Supported by the
Austrian Science Fund (FWF)

Der Wissenschaftsfonds.

SFB sponsors:

- **Austrian Science Fund** (FWF)
- **University of Graz**
- **Graz University of Technology**
- **Medical University of Graz**
- **Government of Styria**
- **City of Graz**

Magnetic Induction Tomography: A feasibility study of brain oedema detection using a finite element human head model

R. Merwa[1] and H. Scharfetter[1]

[1] Institute of Medical Engineering, GrazUniversity ofTechnology, Kronesgasse 5, 8010 Graz, Austria

Abstract—**Neurological aggraviations of patients with craniocerebral injury can trace back in most cases to a swelling of the brain. The survey of these patients is carried out with intracranial pressure sensors in combination with different imaging techniques. This method causes a big distress for the patients, thus new non-invasive methods are required. One promising possibility is magnetic induction tomography, a non-invasive and contactless imaging method for reconstructing the electrical tissue properties in the region of interest. This technique is attractive for the detection of brain oedema, because the magnetic field penetrates easily through the skull and due to the increased fluid accumulation an oedema represents a more or less localized perturbation of the conductivity within a normal brain. We carried out a feasibility study with a 3D arrangement, which comprises a human brain model, an array of 16 excitation coils and 32 receiving coils. The human brain model consists of about 35000 tetrahedral finite elements and considers the cerebrospinal fluid around the brain, the grey matter, the white matter and a spherical oedema. The inverse problem is solved by means of a single step algorithm with four regularization methods and the results show the possibility of the detection of pathological hydration changes with good localization.**

Keywords—**magnetic induction tomography, inverse problem, regularization, finite elements, brain oedema**

I. Introduction

The detection and continuous monitoring of brain oedema is of particular interest in clinical applications because existing methods as invasive measurement of the intracranial pressure may cause big distress for the patients. In this context magnetic induction tomography (MIT) appears attractive. MIT is a noninvasive and contactless imaging method for reconstructing the changes $\Delta\kappa$ of the complex conductivity distribution $\kappa = \sigma + j\omega\epsilon$ in a target object [13], [3], [6]. Magnetically coupled conductivity sensors [10] specifically when applied at multiple frequencies [11], appear attractive for the monitoring of pathologies in the brain, which are correlated with local fluid shifts, e.g. oedema, hemorrhages or epileptic events. To this end a sinusoidal time varying magnetic field B_0 generated by an excitation coil penetrates the object under investigation. Eddy currents are induced, perturbing the primary field B_0. A change $\Delta\kappa$ of the conductivity results in an additional perturbation B of B_0. The corresponding voltages V and V_0 induced in a receiver coil carry the information about the conductivity distribution, which is essential for the solution of the inverse problem.

II. Methods

A. Segmentation

The segmentation of the human brain was performed manually with a custom made software written in Matlab (The MathWorks Inc.). Parametric natural cubic splines are used to interpolate the anatomical boundaries with a low number of base points. The result is a set of points, which describe the geometry in 3D. The outer boundary of the grey matter was extracted from about 150 images of the human head from the Visible Man Human Project database (NPAC/OLDA Visible Human Viewer). The border of the white matter and the cerebrospinal fluid around the brain were not segmented but calculated by assuming a constant thickness of the cerebrospinal fluid and the grey matter.

B. Finite element model

For the generation of models with arbitrary geometry a software package is used consisting of a commercial mesh-generator (HyperMesh, Altair Inc.) and an interactive preprocessing tool written in Matlab (The MathWorks Inc.). This package allows the generation of simple and complex finite element meshes with tetrahedral elements of second order. The information of the geometry is passed to HyperMesh via a command-code which is automatically generated by the preprocessor. This automation avoids the necessity for manual interaction during the meshing process. An additional feature of the preprocessing tool is that it allows the interactive positioning of one or several defined perturbations within a simple or anatomical model (e. g. an oedema in a human brain) and the variation of the structures by means of a special graphical user interface.

Hermann Scharfetter, Robert Merva (Eds.): ICEBI 2007, IFMBE Proceedings 17, pp. 480–483, 2007
www.springerlink.com

C. Forward solver and sensitivity matrix

The boundary value problem is a time harmonic eddy current problem in the steady state described by Maxwell's equations and the associated constitutive laws. This problem is solved with the finite element method whereas the complex A_r,V-A_r formulation was used. The implementation of this finite element forward solver has been described in [8].

In order to solve the inverse problem the sensitivity matrix **S** is required which maps the changes of the conductivity distribution $d\boldsymbol{\kappa}$ onto the changes of the induced voltages $d\boldsymbol{V_i}$ in the receiver channels. The whole formulation of the sensitivity matrix which is an extension of the Geselowitz theorem to the general electromagnetic case has been described in detail in [5].

D. Inverse problem

In order to solve the inverse problem $\boldsymbol{\kappa}$ is generally calculated by means of an iterative scheme. But this process is very time-consuming because of the recalculation of the sensitivity matrix in each iteration step. Thus a Newton-one-step reconstructor [1] is used. Hence if a regularization matrix $\boldsymbol{R}$ and a regularization parameter λ are implemented the inverse solution of the linearized problem is defined as

$$\Delta\boldsymbol{\kappa} = \left(\boldsymbol{S}^T\boldsymbol{S} + \lambda\boldsymbol{R}^T\boldsymbol{R}\right)^{-1}\boldsymbol{S}^T\Delta\boldsymbol{V_i} \qquad (1)$$

whereby $\Delta\boldsymbol{\kappa}$ specify the change of the conductivity between two states and $\Delta\boldsymbol{V_i}$ are the corresponding changes of the induced voltages.

E. Regularization

The inverse problem was calculated with four different regularization methods described in [9]:

a) Unit matrix
b) Variance uniformization
c) Neighbouring matrix
d) Truncated singular value decomposition

The abbreviations of the regularization methods are in the following IM for the unit matrix, VU for the variance uniformization, NM for the neighbouring matrix and TSVD for the truncated singular value decomposition.

Because of using the Newton-one-step reconstructor it is not efficient to calculate the regularization parameter or the truncation level with the method of L-curves. Another well known method is the Morozov criterion discribed in [4]. The idea behind this criterion is that it cannot be expected to obtain less random error in the approximated solution than in the data. In this case the optimal regularization parameter or truncation level in case of truncated singular value decomposition is determined so that

$$Var(\boldsymbol{Noise}_{meas}) = Var(\boldsymbol{S}\Delta\boldsymbol{\kappa_r} - \Delta\boldsymbol{V_i}) \qquad (2)$$

whereas $\Delta\boldsymbol{\kappa}_r$ is the recunstructed distribution of the conductivity changes and $\Delta\boldsymbol{V_i}$ are the induced voltage changes. *Var()* describes the variance of the given term in brackets. The implementation of this method leads to stable images and gives a good basic method in order to compare the different regularization methods. The corresponding regularization parameters for the simulations are listed in table 1

Table 1 Regularization parameter λ and truncation level t for 1 % noise

	IM	VU	NM	TSVD
λ / t	$8.67\ 10^{-21}$	$3.27\ 10^{-10}$	$1.07\ 10^{-21}$	220

F. Simulation arrangement

The 3D arrangement depicted in figure 1 and figure 2 comprises a human brain model with an oedema (spherical perturbation) inside and an array of 16 excitation coils and 32 receiving coils. The excitation coils had a diameter of 60 mm and a height of 18 mm. They were arranged onto a ring with a radius of 85 mm around the brain model. The receiver coils had an edge length of 20 mm and were placed on two parallel rings with a radius of 80 mm. The excitation frequency was 100 kHz and in addition 1 % of the maximum of ΔV due to the perturbation was added to the simulated voltage data as uncorrelated Gaussian noise in order to simulate the noise of the receiver channels. The human head model consists of about 35000 tetrahedral finite elements and considers the cerebrospinal fluid around the brain, the grey matter, the white matter and a spherical oedema. The thickness of the cerebrospinal fluid and the grey matter was set to 8 mm, and the spherical perturbation with a radius of 20 mm was placed inside the white matter. In table 2 the number of finite elements and the tissue parameters of the used structures are listed.

To obtain the conductivity and the relative permittivity of different tissue types at defined frequencies the parametric model described in [2] was used. The oedema was assumed to be extracellular, hence increasing the conductivity at low frequencies. Exact tissue parameters of an extracellular oedema are not well established in the literature, hence they were assumed with the help of the measurement results for an intracellular oedema published in [7]. The central hypothesis is that the β-dispersion changes in a characteristic

Table 2 Number of finte elements and tissue parameters of the used brain structure

Structure	Number of FEs	$\sigma(Sm^{-1})$	ϵ_r
Cerebrospinal fluid	14000	1.6	200
Grey matter	9500	0.134	3222
White matter	11000	0.082	2107
Perturbation	1200 0.164	1000	

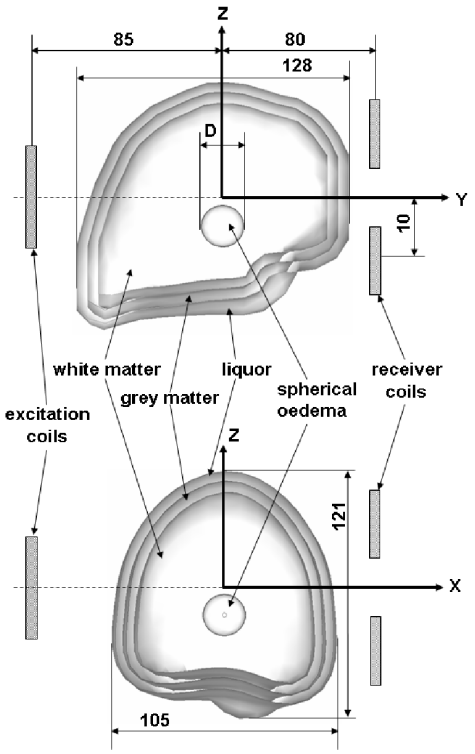

Fig. 1 Simulation arrangement for solving the inverse problem and generating simulated measuring data, top: lateral view, down: front view, all measures in mm

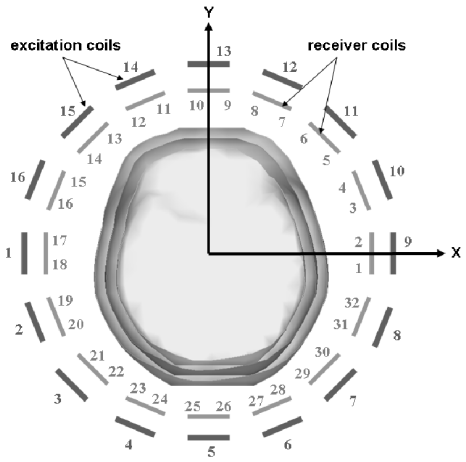

Fig. 2 Top view of the simulation arrangement for solving the inverse problem and generating simulated measuring data

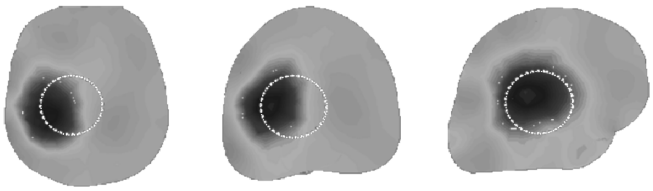

Fig. 3 Reconstruction of $\Delta\kappa$ for the position of the oedema at [x,y,z]=[-10,-10,0] with EM; left: top view, central: front view, right: lateral view

way during a change of the tissue hydration. Accordingly the conductivity of the oedema was assumed as twice the conductivity of the white matter and the relative permittivity was set to about half the value of the white matter.

III. Results

Figure 3 - 6 show the reconstructed images obtained with the four different regularization methods. The regularization parameter and the truncation level were chosen such as listed in table 1. Because of the non- iterative nature of the algorithm the absolute values of the results cannot be interpreted quantitatively, because the first iteration step in (1) yields the correct search direction but usually a wrong step width, due to the lack of a line search. On this account the colormaps were not quantified and only the location and the visual appearance of the reconstructed perturbation were assessed. The white dotted lines in the figures demonstrate the original position of the perturbation.

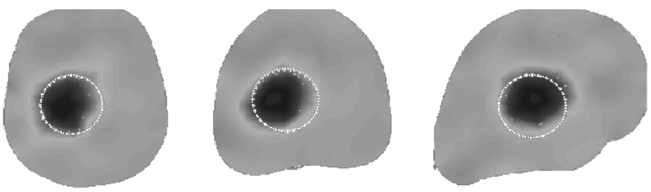

Fig. 4 Reconstruction of $\Delta\kappa$ for the position of the oedema at [x,y,z]=[-10,-10,0] with VU; left: top view, central: front view, right: lateral view

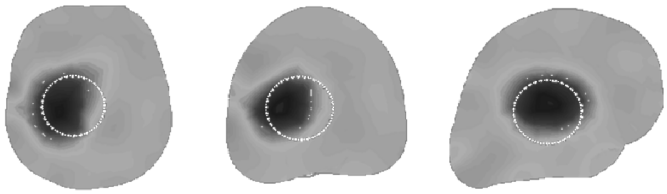

Fig. 5 Reconstruction of $\Delta\kappa$ for the position of the oedema at [x,y,z]=[-10,-10,0] with NM; left: top view, central: front view, right: lateral view

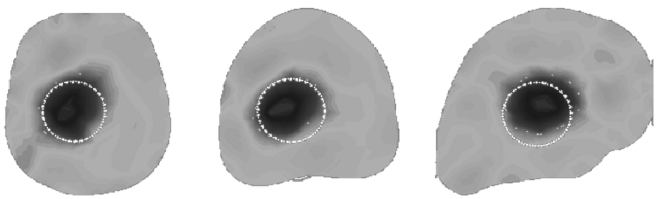

Fig. 6 Reconstruction of $\Delta\kappa$ for the position of the oedema at [x,y,z]=[-10,-10,0] with TSVD; left: top view, central: front view, right: lateral view

IV. Discussion

A 3D finite element human brain model was generated in order to investigate the feasibility of detecting an extracellular oedema inside the brain with MIT. The model comprises the liquor around the brain, the grey matter and the white matter. For the oedema a spherical perturbation was modelled with twice the conductivity of the white matter. The oedema had a radius of 20 mm and first results obtained with 16 excitation coils and 32 receiving coils demonstrate the detectability of injuries in this vein. The required SNR of 40 dB can be achieved with our MIT-system [12] when reducing the sampling bandwidth to abot 0.2 Hz and driving the coils with 1 ampere.

The reconstructed images depicted in the figures 3 - 6 show a good localization of the spherical perturbation inside the white matter. All perturbations are slightly displaced towards the nearest border of the brain whereas this effect is clearly visible in figure 3 and figure 5. This displacement is an inherent property of the point spread function and depends on the amount of regularization obtained with the Morozov criterion. When comparing the regularization schemes, the unit matrix and the variance uniformization approach yield the smoothest solutions. The most homogeneous background is also obtained with variance uniformization, according to the variance constraint based on this regularization scheme. In terms of the displacement of the reconstructed oedema the best results were obtained with the truncated singular value decomposition and with the variance uniformization.

The shown results were obtained at a single frequency only. Future work should concentrate onto the exploitation of the frequency dependence of the tissue conductivity and measurements at frequencies up to several MHz [11]. Multifrequency measurements can decrease the degree of ill-conditioning of the inverse problem if additional a-priori information is included in form of spectral tissue models.

Acknowledgment

This work was supported by the Austrian Science Foundation SFB, project F32N18.

References

1. Cheney M, Isaacson D, Newell J C, Simske S and Goble J (1990) NOSER: An algorithm for solving the inverse conductivity problem. Int. J. Imag. Syst. Tech. 2:66–75
2. Gabriel S, Lau R W, Gabriel C (1996) The dielectric properties of biological tissues: III. Parametric models for the dielectric spectrum of tissues. Phys. Med. Biol. 41:2271–2293
3. Griffiths H 2001 Magnetic induction tomography. Meas. Sci. Technol. 12:1126–1131
4. Hansen P C (1998) Rank-deficient and ill-posed problems. Siam
5. Hollaus K, Magele C, Merwa R and Scharfetter H (2004) Fast calculation of the sensitivity matrix in magnetic induction tomography by tetrahedral edge finite elements and the reciprocity theorem. Physiol. Meas. 25:159–168
6. Korjenevsky A, Cherepenin V and Sapetsky S (2000) Magnetic induction tomography: experimental realization. Physiol. Meas. 21: 89–94
7. Lingwood B, Dunster K, Colditz P and Ward L (2002) Noninvasive measurement of cerebral bioimpedance for detection of cerebral edema in the neonatal piglet. Brain Research 954:97–105
8. Merwa R, Hollaus K, Brandsttter B and Scharfetter H (2003) Numerical solution of the general 3D eddy current problem for magnetic induction tomography (spectroscopy). Physiol. Meas. 24:545–554
9. Merwa R, Hollaus K and Scharfetter H (2005) Solution of the inverse problem of magnetic induction tomography (MIT). Physiol. Meas. 26:241–250
10. Netz J, Forner E and Haagemann S (1993) Contactless impedance measurement by magnetic induction - a possible method for investigation of brain impedance. Physiol. Meas. 14:463–471
11. Scharfetter H, Casanas R and Rosell J (2003) Biological tissue characterization by magnetic induction spectroscopy (MIS): requirements and limitations. IEEE. Trans. Biomed. Eng. 50:870–880
12. Scharfetter H, Kstinger A and Issa S (2007) Spectroscopic 16 channel magnetic induction tomograph: The new Graz MIT system. This issue
13. Tapp H and Peyton A (2003) A State of the Art Review of Electromagnetic Tomography. Proc. 3rd world congress on industrial process tomography 340–346

Address of the corresponding author:
Author: Robert Merwa
Institute: Institute of Medical Engineering
Street: Kronesgasse 5
City: Graz
Country: Austria
Email: merwa@tugraz.at